

Article

A High-Efficiency Cooperative Control Strategy of Active and Passive Heating for a Proton Exchange Membrane Fuel Cell

Chunjuan Shen ^{1,2}, Sichuan Xu ¹, Lei Pan ¹ and Yuan Gao ^{1,*}

¹ School of Automotive Studies, Tongji University, Shanghai 201804, China; cjshen@alumni.tongji.edu.cn (C.S.); scxu@tongji.edu.cn (S.X.); lp18114862036@163.com (L.P.)

² Shanghai Ranrui New Energy Vehicle Technology Co., Ltd., Shanghai 201804, China

* Correspondence: yuangao@tongji.edu.cn; Tel.: +86-(0)-18601736046

Abstract: The key to overcome PEMFC cold start failure is to raise the stack temperature above 0 °C before the electrochemical reaction. As the electrochemical reaction progresses, reaction heat is released inside the stack, which will heat the PEMFC stack. This heating method is called passive heating, referred to as PH in this article. Another method, called active heating, or simplified to AH in this article, involves artificially adding a device to the stack to input extra heat to the stack to increase the stack temperature more quickly and reduce the icing rate of the stack water. In this study, an optimal cooperative control strategy of AH and PH is explored by integrating AH and PH. The most effective cold start can be achieved when the temperature of the stack is raised to −20 °C by using AH with the reaction heat of the stack itself. This study provides guidance for optimizing the cold start performance of a PEMFC.

Keywords: cooperative control strategy; effective cold start; integrating active heating; PEMFC stack



Citation: Shen, C.; Xu, S.; Pan, L.; Gao, Y. A High-Efficiency Cooperative Control Strategy of Active and Passive Heating for a Proton Exchange Membrane Fuel Cell. *Energies* **2021**, *14*, 7301. <https://doi.org/10.3390/en14217301>

Academic Editor: Ricardo J. Bessa

Received: 1 September 2021

Accepted: 19 October 2021

Published: 4 November 2021

Publisher's Note: MDPI stays neutral with regard to jurisdictional claims in published maps and institutional affiliations.



Copyright: © 2021 by the authors. Licensee MDPI, Basel, Switzerland. This article is an open access article distributed under the terms and conditions of the Creative Commons Attribution (CC BY) license (<https://creativecommons.org/licenses/by/4.0/>).

1. Introduction

With a decline in fossil energy reserves and the aggravation of environmental pollution in the world, human beings have to accelerate the process of energy conversion. For this reason, researchers need to work harder to find a more environmentally friendly alternative energy to reduce the use of fossil energy. The transportation industry is one of the highest consumers of oil and it causes serious environmental pollution every year [1]. Therefore, accelerating the process of energy conversion in the transportation industry would make a significant contribution to world energy transformation and environmental protection. Research on new energy vehicles started as early as the end of the 20th century, and, in recent years, has achieved great progress. Pure electric vehicles and fuel cell vehicles have both begun their commercialization process [2]. The PEMFC has become one of the most promising development paths for new energy vehicles, due to its highly efficient energy conversion rate and clean reaction products. Meanwhile, because a PEMFC can work at a relatively low temperature and still maintain its high energy conversion rate, it has become a more economical power source when applied in vehicles [3].

However, there are many problems associated with the application of PEMFCs in electric vehicles, such as their durability and the low-temperature cold start problem of PEMFC vehicles which urgently needs to be solved and is the most studied problem.

A PEMFC low-temperature cold start, as the name implies, refers to starting a vehicle quickly and stably when the ambient temperature is below 0 °C, usually between −10 and −30 °C. However, since the energy source used in a PEMFC is hydrogen and its reaction product is water, it will quickly condense into ice at extremely low temperatures, which will block the gas diffusion layer, cover the surface of the catalytic layer, and then reduce the reaction activation area [4]. Before the reaction activation surface area is reduced to zero, if the temperature of the fuel cell is still not above 0 °C, the electrochemical reaction will stop, leading to the fuel cell's cold start failure [5]. Therefore, in order to ensure the

success of PEMFC low-temperature cold start, the temperature of a PEMFC must be above 0 °C before ice completely blocks the pores of the catalytic layer [6].

In order to start a PEMFC successfully in a low temperature environment, Luo et al. [7] studied the mechanism of cell cold start in detail through a variety of experiments, and systematically explained the reasons for cold start failure from the aspects of materials, reaction process, and so on. Wu et al. [8] found that the degradation of PEMFC internal materials caused the decline in fuel cell performance under the condition of cold start. On this basis, Knorr et al. [9] proposed that the use of methanol as an antifreeze for vehicles parked in a low temperature environment could prevent the degradation of PEMFC performance. However, further research found that when methanol was used as an antifreeze, the PEMFC performance at room temperature was worse. Jiang et al. [10] and Ko et al. [11] studied the effect of current density on cold start performance. They believed that increasing the initial current density accelerated the temperature rise of the fuel cell, and increased the water accumulation in the cathode catalytic layer, which could easily lead to the cold start failure. Therefore, Amamou et al. [12] proposed a real-time adaptive cold start strategy for a fuel cell to control the running current in real time and quickly cold start the fuel cell. Li [13] and Yang [14] et al. further studied the influence of current density on battery performance and found that, during cold start, a higher starting current density increased the freezing probability in a fuel cell. Therefore, reducing the starting current density can improve the cold start capability of fuel cells.

At the same time, many scientists have studied the heating methods of a PEMFC. In [15] and [16] the authors clarified that although a PEMFC can generate more heat energy when operating at room temperature, it is difficult to achieve a successful cold start by increasing the temperature of the stack with the heat generated by the electrochemical reaction when the ambient temperature is low. Therefore, researchers have come up with many methods of AH. Zhang et al. [17] put forward a heating method for a PEMFC by adding a circulating heating medium around the fuel cell. On this basis, Li et al. [18] proposed a method of wrapping thermal insulation material around the fuel cell stack and circulating a heating medium during cold start to preheat the stack. However, due to the addition of a layer of medium which must be heated while heating the stack, the heat energy consumption was significantly increased and the cost was higher, although the heating effect was obvious. Khandelwal et al. [19] found that during cold start, the temperature distribution in a PEMFC was significantly affected by the heat capacity and thermal conductivity of each component. Zalba et al. [20] proposed a phase change material that could store a large amount of latent heat and could be used as a miniature heat transfer material. Therefore, for short-time shutdown of a fuel cell, the phase change latent heat could be used as a heat source. Using a numerical calculation, Sasmito et al. [21] also found that when phase change materials were used as the heat storage medium, the fuel cell stack could be successfully started at −20 °C. Li et al. [22] proposed a local heating method, in which the heating wire was placed under part of the ridge of the cathode plate, and the heating effect was also significantly improved.

Although there are a variety of AH methods with both good and bad effects, there is no further study on how to properly use AH methods [23], which means how to coordinate AH and PH. Thus, in this study, we propose three different cooperative control strategies of AH and PH, and through experiments of two different PEMFC stacks, we analyze the cold start time and the performance of the stack during start-up in the experiment, and summarize a set of optimal fuel cell cold start strategies. The purpose of this study is to explore the best performance of a fuel cell during cold start in constant current mode on the basis of experiments. According to this study, we can determine an optimal constant current cold start strategy, and can identify the shortcomings of constant current cold start as compared with other cold start strategies. In order to draw these conclusions, we have carried out experiments on two different PEMFC stacks, Stack A made in China and Stack B made in Germany.

2. Experiment

2.1. Preparation before the Experiment

In order to make the experimental results more reliable, two different PEMFC stacks were used as the control experiment in this study. They are Stack A made in China and Stack B made in Germany.

The main components of the test bench included a BOP set of components (such as an air compressor, humidifier, back pressure valve, ejector, tail row solenoid valve, cooling water pump, thermostat, PTC heater, FCU, and DCDC) suitable for a 30 kW fuel cell system, and a PTC heater was used for AH. In addition, it also included a heat dissipation system and an electronic load.

The main parameters of Stack A are shown in Table 1, the main parameters of Stack B are shown in Table 2, and the test bench for this experiment is shown in Figure 1.

Table 1. Basic parameters of Stack A.

Item	Unit	Value
Voltage	V	100~220
Current	A	0~364
Rated voltage	V	132
Rated current	A	273
Rated power	kW	36
Effective membrane area	cm ²	227
Number of pieces		220

Table 2. Basic parameters of Stack B.

Item	Unit	Value
Voltage	V	100~240
Current	A	0~350
Rated voltage	V	160
Rated current	A	225
Rated power	kW	36
Effective membrane area	cm ²	190
Number of pieces		240

Before the experiment, first, the two tested stacks were operated stably for a certain period of time to simulate the status of the stacks of actual vehicles after running. After that, the bench went into the shutdown and purge process. In order to keep consistent with the working condition of actual vehicles, anode and cathode reaction gases were used to purge the stacks, in which the stoichiometric ratio of hydrogen and air was 1.5:4.5. The result of purging was to ensure that the inner flow channel of the stack was dry and the proton exchange membrane had a proper degree of wetting [24]. After purging, the experimental stacks were placed in an environment of $-30\text{ }^{\circ}\text{C}$ for 12 h for cooling. The cooling method involved putting the PEMFC into a refrigerator in which the temperature was $-30\text{ }^{\circ}\text{C}$ and stewing for 12 h. It was possible that the temperature of the refrigerator fluctuated within $1\text{ }^{\circ}\text{C}$, but it did not matter.



Figure 1. The test bench for the experiment.

2.2. Method

Before the experiment, we tested whether the cooling water temperature of the stack was $-30\text{ }^{\circ}\text{C}$. If the experimental temperature was $-30\text{ }^{\circ}\text{C}$, the experiment was started.

The first step was to start up the PEMFC stack according to a normal start-up process and turn on the PTC electric heater. A PTC electric heater was used to heat the cooling water circuit to raise the temperature of the stack. Control Strategy 1 increased the temperature to $-15\text{ }^{\circ}\text{C}$, control Strategy 2 increased the temperature to $-20\text{ }^{\circ}\text{C}$, and control Strategy 3 increased the temperature to $-25\text{ }^{\circ}\text{C}$, and then the second step is executed.

The second step was to judge whether the AH was completed through the temperature. If the temperature of the cooling water circuit reached the required temperature of the control strategy, the third step was executed.

The third step was to turn off the PTC electric heater, keep the stack starting stably, and then execute the fourth step.

The fourth step was to observe whether the stack temperature reached $0\text{ }^{\circ}\text{C}$. If it reached $0\text{ }^{\circ}\text{C}$ successfully, the fifth step was executed. Otherwise, we went back to the first step and carries out the cold start experiment again. The time, T_1 , from the stack startup to the stack temperature reaching $0\text{ }^{\circ}\text{C}$ was recorded, and the fifth step was executed.

The fifth step was to maintain the output power of the PEMFC stack, observe its power change, and then execute the sixth step.

The sixth step was to keep the stack working stably at the rated power for ten minutes. Then, the stack was turned off, and the cold start experiment was completed.

In order to verify the reproducibility of the results, this experiment was carried out twice with two different PEMFC stacks, which confirmed the repeatability of the cold start characteristics under the same parameters, as well as the uncorrelated quantitative difference between the two tests at a PEMFC system level.

3. Results and Discussion

3.1. Stack Temperature

In the whole study of the control strategy, the cold start rate of the PEMFC is a key index for evaluating the cold start performance, and the speed of a cold start experiment is reflected by the rate of change of the PEMFC stack temperature. Figures 2 and 3 show the graphs of the temperature change in Stack A and in Stack B with time under the conditions of control Strategy 1, control Strategy 2, and control Strategy 3, respectively.

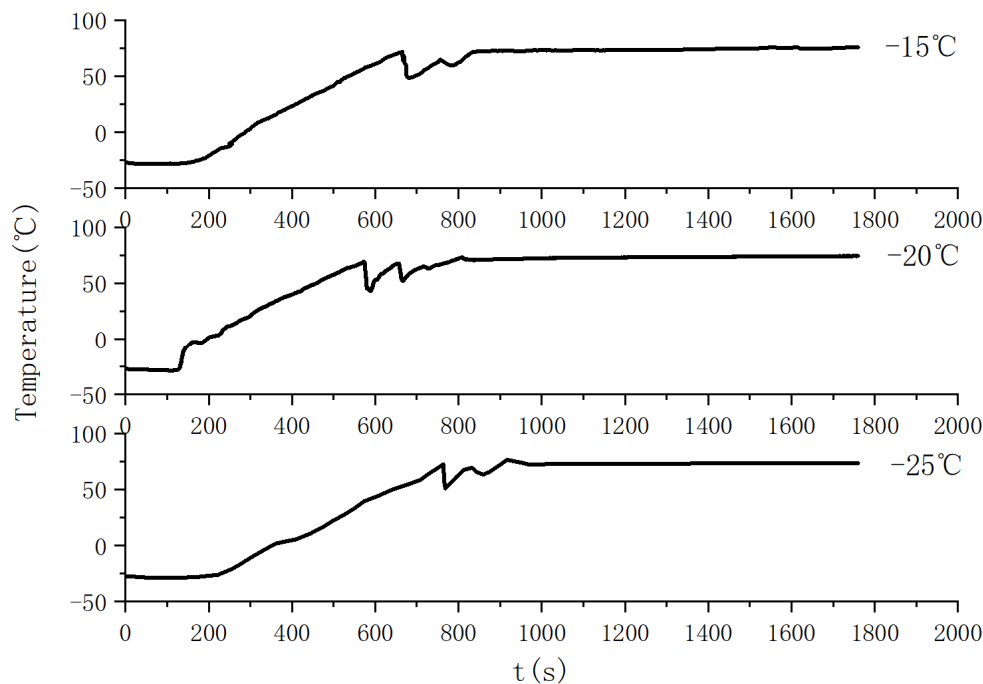


Figure 2. Graph of the temperature change in Stack A with time.

Two key data are shown in the figures, which are the elapsed time, T_a , when the stack temperature rises from the starting temperature to 0 °C and the elapsed time, T_b , when the stack temperature rises from 0 °C to the stable temperature. Generally, when the temperature in the PEMFC stack reaches 0 °C, it indicates the success of the cold start [25]. Since each group of experiments is carried out at a cold start temperature of -30 °C and the temperature change range is consistent, the parameter T_a can be used to analyze the speed of cold start directly. The elapsed time from 0 °C to the stable temperature, that is, the time required for the stack to output power at full capacity after reaching 0 °C until the stack reaches steady state, also affects the rate of subsequent active chemical reaction in the stack due to the fact that the internal structure of the stack may have different changes with different control strategies [26], and therefore it can be judged by parameter T_b .

3.1.1. Parameter T_a

For Stack A, it can be seen from the figure that the values of the parameter T_a are $T_{Xa1} = 468$ s, $T_{Xa2} = 196$ s, and $T_{Xa3} = 530$ s under control Strategy 1, control Strategy 2, and control Strategy 3, respectively; for Stack B, it can also be seen from the figure that $T_{Ea1} = 297$ s, $T_{Ea2} = 167$ s and $T_{Ea3} = 322$ s. By comparing the numerical values, it can be seen that Stack A and Stack B show the same results, that is, the cold start rate of control Strategy 2 is much higher than that of control Strategy 1 and control Strategy 3, and the cold start rate of control Strategy 1 is slightly higher than that of control Strategy 3. The reason can be analyzed from the figure, which shows that when the stack is heated to -25 or -15 °C by the PTC electric heating, the PEMFC stack presents a longer period of time when it is stable at the starting temperature of -30 °C than when it is heated to -20 °C [27].

During this period of time, the electrochemical reaction in the fuel cell stack is very slow, and the temperature rise rate of the stack is also lower, which directly extend the cold start time of the PEMFC stack.

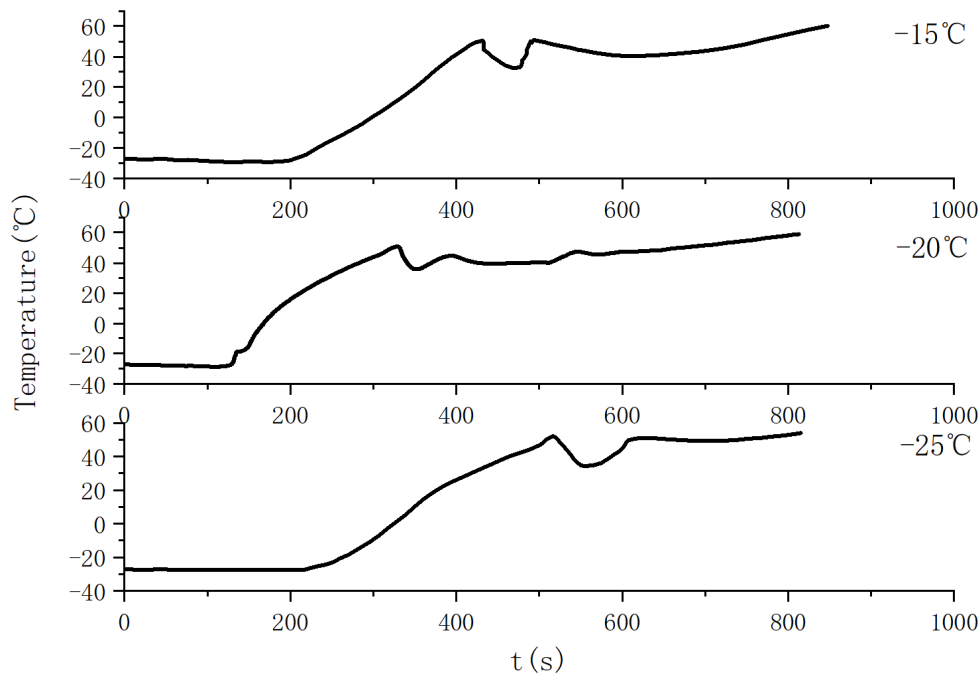


Figure 3. Graph of the temperature change in Stack B with time.

3.1.2. Parameter T_b

It can be seen from the temperature change curves in Figures 2 and 3 that the results of using different stacks and different strategies are significantly different. In Stack A, the PEMFC stack experiment with the control Strategies 1, 2, and 3 reach a stable temperature at 1022, 815, and 1033 s, respectively, which means that the elapsed times from 0 °C to the stable temperature are $T_{Xb1} = 554$ s, $T_{Xb2} = 619$ s, and $T_{Xb3} = 503$ s, respectively. In Stack B, the PEMFC stack experiment with the three control Strategies 1, 2, and 3 reach a stable temperature at 619, 424, and 615 s, which means that the elapsed times from 0 °C to the stable temperature are $T_{Eb1} = 322$ s, $T_{Eb2} = 257$ s, $T_{Eb3} = 293$ s. By analyzing these data, it is easily found that, although the parameter T_b is different under various control strategies, the variation range is not large and the difference does not have regularity, therefore, on the one hand, the experimental conditions under different control strategies have no obvious effect on the active chemical reaction of the stack after 0 °C. On the other hand, it shows that the ability of the PEMFC to overcome ice formation inside the stack in a low temperature environment is mainly affected by the AH of the stack with the PTC electric heater during the cold start experiment.

3.2. Stack Power

Figures 4 and 5 show the variation curves of the output power of Stack A and Stack B, respectively, with time.

Among the contents studied in this paper, an important index to evaluate the proposed cold start control strategy of a PEMFC stack is the change in stack power. In this study, in Stack A, the half-rated power is $P_{XI} = 18$ kW and the rated power is $P_{XE} = 36$ kW; in Stack B, the half-rated power is $P_{EI} = 18$ kW and the rated power is $P_{EE} = 36$ kW. Since the inherent performance of the stack itself is certain [28], the focus of all discussions in this study is the time required for the PEMFC stack to reach the inherent power of the stack itself after the cold start. In this study, two parameters are used to evaluate the performance

of the stack, which are time T_I from start-up to half-rated power (50% power) and time T_E from half-rated power to rated power.

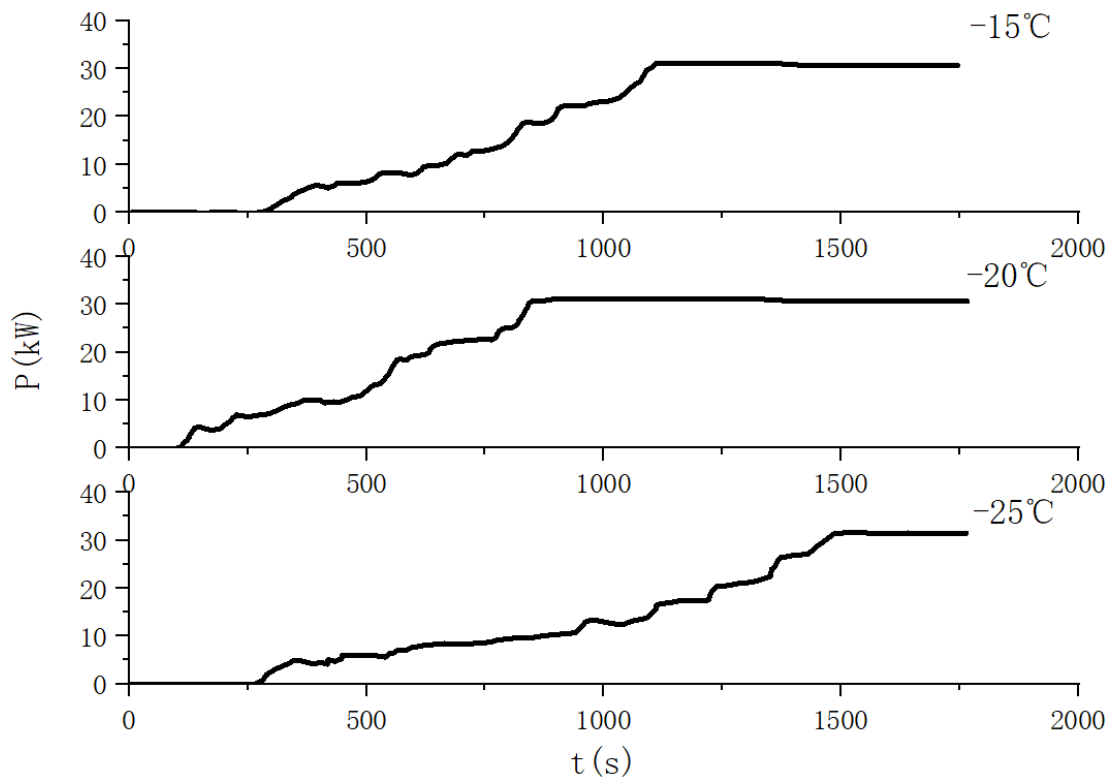


Figure 4. Graph of the power change in Stack A with time.

3.2.1. Parameter T_I

After the complex cold start process, the PEMFC stack reaches a critical point where it can gradually heat up through the heat release of its own electrochemical reaction and steadily increase the output power. This critical state is usually called half-rated state, and the output power of the stack in this state is called half-rated power. Since the most important and complicated process of cold start is the start-up process of the stack below $0\text{ }^{\circ}\text{C}$, and this process is included in the stage from start-up to idle power [29], the cold start performance of the PEMFC stack can be analyzed by T_I .

For Stack A, the time from start-up to half-rated power of the PEMFC stack under the three control strategies is $T_{XI1} = 825\text{ s}$, $T_{XI2} = 560\text{ s}$, and $T_{XI3} = 1122\text{ s}$. From the numerical comparison of T_I , it is obvious that in the experiment of control Strategy 2, the PEMFC stack reaches the half-rated power more quickly. This is the same as the time required to rise from the start-up temperature to $0\text{ }^{\circ}\text{C}$ mentioned above, which shows that the PEMFC achieves a better effect of cold start under the condition of control Strategy 2. The difference is that the time T_a required to rise from the start-up temperature to $0\text{ }^{\circ}\text{C}$ evaluates the quality of the cold start from the state of the stack itself, and the time T_I from start-up to the half-rated power reflects the quality of the cold start from the output performance [30]. Of course, this only evaluates the impact of different control strategies on Stack A. Next, we discuss the performance of Stack B. For Stack B, Figure 5 shows a similar result to that of Stack A under the same three control strategies. The time from start-up to half-rated power is $T_{EI1} = 430\text{ s}$, $T_{EI2} = 315\text{ s}$, and $T_{EI3} = 410\text{ s}$, that is, the PEMFC reaches the half-rated power faster under control Strategy 2, which also verifies the conclusion drawn in Stack A, i.e., under the condition of control Strategy 2, the PEMFC achieves a better effect of cold start.

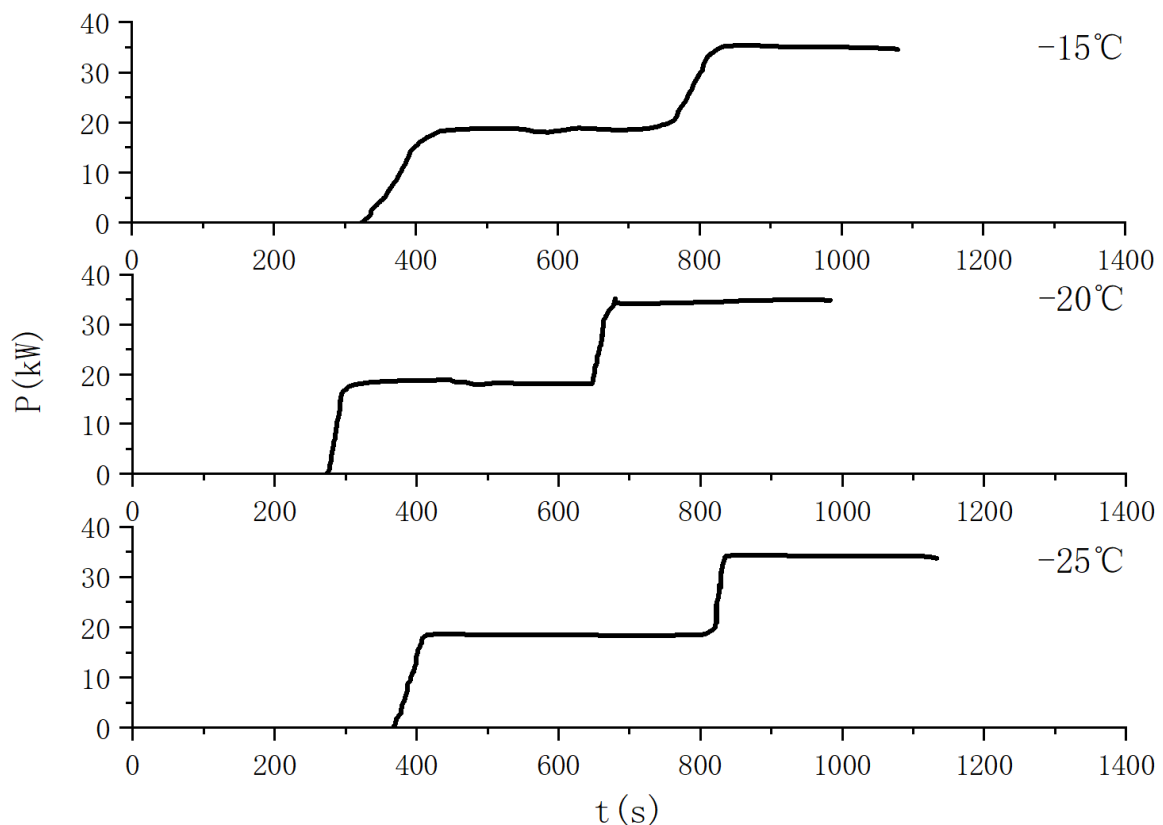


Figure 5. Graph of the power change in Stack B with time.

3.2.2. Parameter T_E

When discussing the time from half-rated power to rated power, we consider the T_E values of the two stacks under different control strategies, as shown in Table 3.

Table 3. T_E values of the two stacks under different control strategies.

	Control Strategy 1	Control Strategy 2	Control Strategy 3
Stack A	$T_{XE1} = 285$ s	$T_{XE2} = 330$ s	$T_{XE3} = 365$ s
Stack B	$T_{EE1} = 411$ s	$T_{EE2} = 365$ s	$T_{EE3} = 432$ s

Among the parameters of the PEMFC stack, rated power is a very important parameter; only when the stack outputs power at the rated power, can the maximum power be provided [31]. Therefore, it is crucial to consider the influence of different control strategies on the speed of the PEMFC stack to reach the rated power. As can be seen from Table 3, both Stack A and Stack B under control Strategy 2 are the fastest to increase the power to the rated power, and, although control Strategies 1 and 3 are different in speed, they both show worse performances as compared with control Strategy 2. Therefore, it can be concluded that control Strategy 2 is the control strategy that can make the stack output the maximum power the fastest [32].

3.3. Monomer Stability

At the end of this section, we evaluate the advantages and disadvantages of each control strategy based on the monomer stability of the stack under the three control strategies. In the experiment, the average monomer voltage of the stack at each time and the lowest monomer voltage are recorded, for each control strategy, and the difference between the two reflects the fluctuation of the monomer voltage of the stack [33]. Therefore, whether the monomer voltage of the stack can quickly stabilize is also an important index

of the performance of the stack. Figures 6 and 7 show the graphs of the monomer stability change in Stack A and Stack B, respectively, with time.

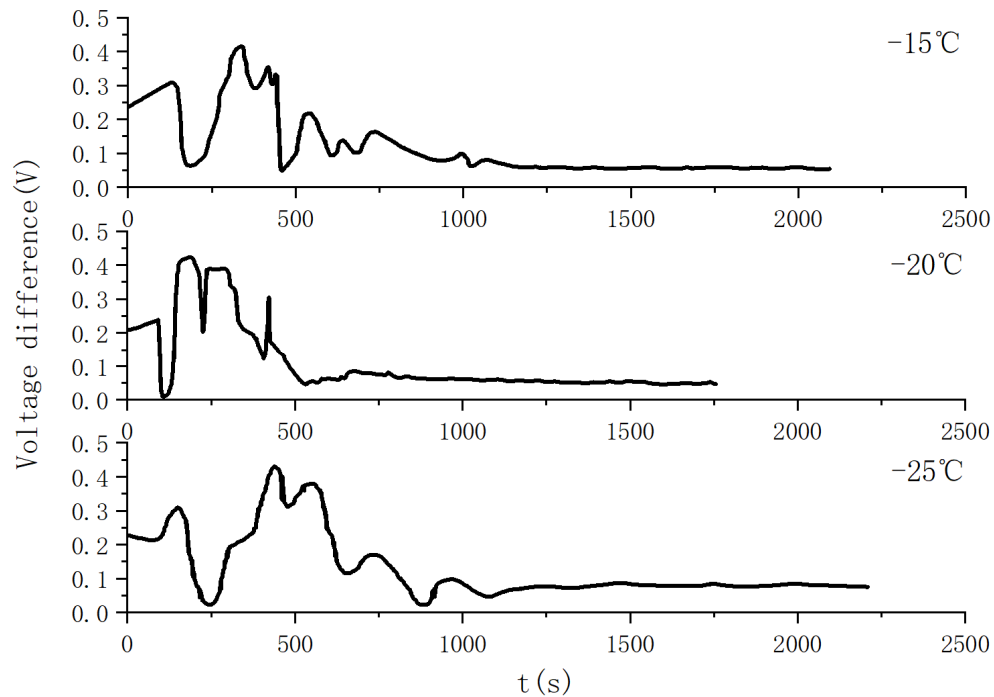


Figure 6. Graphs of the voltage difference change in Stack A with time.

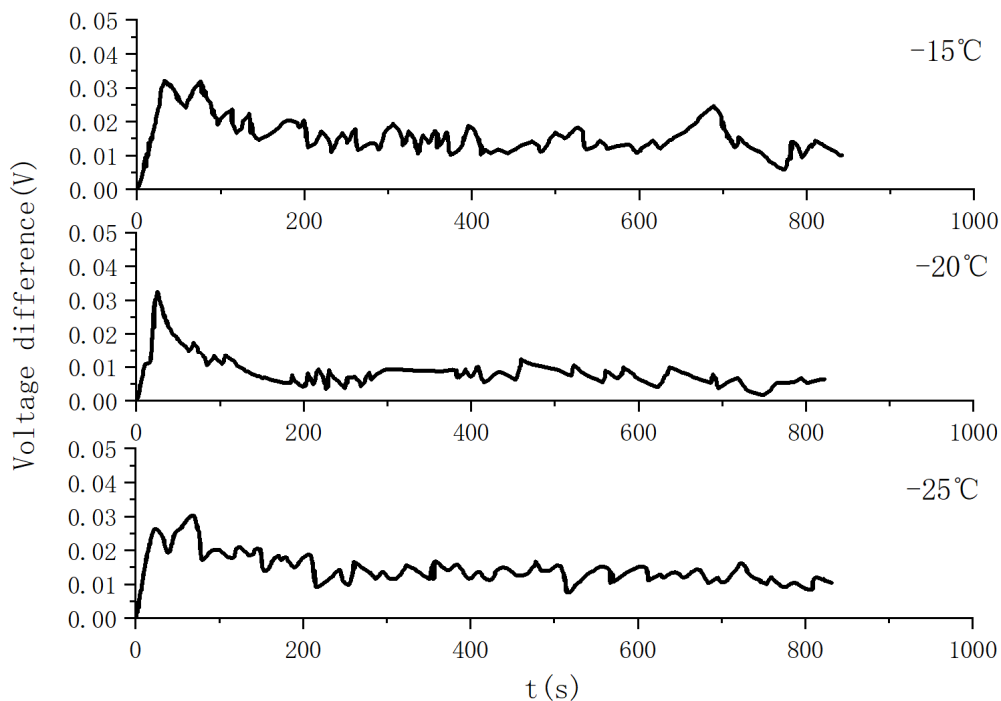


Figure 7. Graphs of the voltage difference change in Stack B with time.

According to the analysis of the graph shown in Figure 6, the difference between the average monomer voltage and the lowest monomer voltage of Stack A during the start-up state of cold start is large, and there are sharp fluctuations. Under the three strategies, the monomer differences of the stack reach the stable state at 1148, 676, and 1183 s, respectively, and the stable differences under each control strategy are 0.06, 0.06, and 0.07 V, respectively,

when reaching the stable state. For Stack B, it can be seen from Figure 7 that the difference between the average monomer voltage and the lowest monomer voltage is small, and the stack reaches the stable state at about 200 s under the three control strategies. Although the speed at which Stack B reaches stability under each control strategy is not very different, there are some differences in the monomer difference when reaching stability: The stable monomer difference of control Strategy 1 is about 0.015 V, that of control Strategy 2 is 0.009 V, and that of the control strategy 3 is 0.013 V. It can be seen that the PEMFC Stack A started under control Strategy 2 and achieved the stable state more quickly, and Stack B showed a smaller change range of monomer voltage [34].

4. Conclusions

In this study, the cold start performance of PEMFC stacks with three different cold start strategies are studied. The cold start experiments are carried out with two different stacks, Stack A and Stack B, in order to make the research results more convincing. This study determines an optimal strategy of cold start by analyzing the cold start time, cold start power, stack polarization curve, and monomer stability under different strategies, that is, when starting the PEMFC stack at an ambient temperature of $-30\text{ }^{\circ}\text{C}$, and actively heating the stack (using a PTC electric heater to heat the stack) at the beginning of cold start until the stack temperature reaches $-20\text{ }^{\circ}\text{C}$, and then turning off the electric heater, the PEMFC stack can stably complete the cold start, and shows the optimal cold start performance and output performance.

This study is an important supplement to the international research on cold start of a PEMFC. It provides an in-depth study of the synergy between AH and PH during cold start, and proposes an effective cooperative control strategy of AH and PH, which may be helpful for further research on cold start in the future.

Author Contributions: Conceptualization: C.S., L.P.; methodology: C.S.; validation, C.S., L.P., Y.G.; formal analysis: C.S.; writing—original draft preparation, C.S.; writing—review and editing, L.P. and Y.G.; supervision: S.X. All authors have read and agreed to the published version of the manuscript.

Funding: This research is supported by the National Key R&D Program of China, no. 2018YFE0105000.

Institutional Review Board Statement: Not applicable.

Informed Consent Statement: Not applicable.

Data Availability Statement: Not applicable.

Conflicts of Interest: The authors declare no conflict of interest.

References

1. Yu, Y.; Li, H.; Wang, H.J.; Yuan, X.Z.; Wang, G.J.; Pan, M. A review on performance degradation of proton exchange membrane fuel cells during startup and shutdown processes: Causes, consequences, and mitigation strategies. *J. Power Sources* **2012**, *205*, 10–23. [[CrossRef](#)]
2. Thomas, C.E. Fuel cell and battery electric vehicles compared. *Int. J. Hydrog. Energy* **2009**, *34*, 6005–6020. [[CrossRef](#)]
3. Jayakumar, A.; Sethu, S.P.; Ramos, M.; Robertson, J.; Al-Jumaily, A. A technical review on gas diffusion, mechanism and medium of PEM fuel cell. *IONICS* **2015**, *21*, 1–18. [[CrossRef](#)]
4. Lee, Y.; Kim, B.; Kim, Y.; Li, X.G. Effects of a microporous layer on the performance degradation of proton exchange membrane fuel cells through repetitive freezing. *J. Power Sources* **2011**, *196*, 1940–1947. [[CrossRef](#)]
5. Ahluwalia, R.K.; Wang, X. Rapid self-start of polymer electrolyte fuel cell stacks from subfreezing temperatures. *J. Power Sources* **2006**, *162*, 502–512. [[CrossRef](#)]
6. Thompson, E.L.; Jorne, J.; Gasteiger, H.A. Oxygen reduction reaction kinetics in subfreezing PEM fuel cells. *J. Electrochem. Soc.* **2007**, *154*, B783–B792. [[CrossRef](#)]
7. Luo, Y.Q.; Jiao, K. Cold start of proton exchange membrane fuel cell. *Prog. Energy Combust.* **2018**, *64*, 29–61. [[CrossRef](#)]
8. Wu, F.; Chen, B.; Pan, M. Degradation of the Sealing Silicone Rubbers in a Proton Exchange Membrane Fuel Cell at Cold Start Conditions. *Int. J. Electrochem. Sci.* **2020**, *15*, 3013–3028. [[CrossRef](#)]
9. Knorr, F.; Sanchez, D.G.; Schirmer, J.; Gazdzicki, P.; Friedrich, K.A. Methanol as antifreeze agent for cold start of automotive polymer electrolyte membrane fuel cells. *Appl. Energy* **2019**, *238*, 1–10. [[CrossRef](#)]

10. Jiang, F.M.; Wang, C.Y.; Chen, K.S. Current Ramping: A Strategy for Rapid Start-up of PEMFCs from Subfreezing Environment. *J. Electrochem. Soc.* **2010**, *157*, B342–B347. [[CrossRef](#)]
11. Ko, J.; Ju, H. Comparison of numerical simulation results and experimental data during cold-start of polymer electrolyte fuel cells. *Appl. Energy* **2012**, *94*, 364–374. [[CrossRef](#)]
12. Amamou, A.; Kandidayeni, M.; Boulon, L.; Kelouwani, S. Real time adaptive efficient cold start strategy for proton exchange membrane fuel cells. *Appl. Energy* **2018**, *216*, 21–30. [[CrossRef](#)]
13. Jia, L.; Tan, Z.T.; Kang, M.; Zhang, Z.Q. Experimental investigation on dynamic characteristics of proton exchange membrane fuel cells at subzero temperatures. *Int. J. Hydrog. Energy* **2014**, *39*, 11120–11127. [[CrossRef](#)]
14. Lin, R.; Weng, Y.M.; Li, Y.; Lin, X.W.; Xu, S.C.; Ma, J.X. Internal behavior of segmented fuel cell during cold start. *Int. J. Hydrog. Energy* **2014**, *39*, 16025–16035. [[CrossRef](#)]
15. Reddy, E.H.; Jayanti, S. Thermal management strategies for a 1 kWe stack of a high temperature proton exchange membrane fuel cell. *Appl. Therm. Eng.* **2012**, *48*, 465–475. [[CrossRef](#)]
16. Jiao, K.; Alaefour, I.E.; Karimi, G.; Li, X.G. Simultaneous measurement of current and temperature distributions in a proton exchange membrane fuel cell during cold start processes. *Electrochim. Acta* **2011**, *56*, 2967–2982. [[CrossRef](#)]
17. Zhang, C.Z.; Yu, T.; Yi, J.; Liu, Z.T.; Raj, K.A.R.; Xia, L.C.; Tu, Z.K.; Chan, S.H. Investigation of heating and cooling in a stand-alone high temperature PEM fuel cell system. *Energy Convers. Manag.* **2016**, *129*, 36–42. [[CrossRef](#)]
18. Youcai, L.; Sichuan, X.; Zhigang, Y.; Yongxiang, L. Experiment and Simulation Study on Cold Start of Automotive PEMFC. In Proceedings of the 2011 International Conference on Electric Information and Control Engineering, Wuhan, China, 15–17 April 2011; pp. 2166–2170.
19. Khandelwal, M.; Lee, S.H.; Mench, M.M. One-dimensional thermal model of cold-start in a polymer electrolyte fuel cell stack. *J. Power Sources* **2007**, *172*, 816–830. [[CrossRef](#)]
20. Zalba, B.; Marin, J.M.; Cabeza, L.F.; Mehling, H. Review on thermal energy storage with phase change: Materials, heat transfer analysis and applications. *Appl. Therm. Eng.* **2003**, *23*, 251–283. [[CrossRef](#)]
21. Sasmito, A.P.; Shamim, T.; Mujumdar, A.S. Passive thermal management for PEM fuel cell stack under cold weather condition using phase change materials (PCM). *Appl. Therm. Eng.* **2013**, *58*, 615–625. [[CrossRef](#)]
22. Li, L.J.; Wang, S.X.; Yue, L.K.; Wang, G.Z. Cold-start method for proton-exchange membrane fuel cells based on locally heating the cathode. *Appl. Energy* **2019**, *254*, 113716. [[CrossRef](#)]
23. Yang, Z.R.; Du, Q.; Jia, Z.W.; Yang, C.G.; Jiao, K. Effects of operating conditions on water and heat management by a transient multi-dimensional PEMFC system model. *Energy* **2019**, *183*, 462–476. [[CrossRef](#)]
24. Zhang, G.B.; Jiao, K. Multi-phase models for water and thermal management of proton exchange membrane fuel cell: A review. *J. Power Sources* **2018**, *391*, 120–133. [[CrossRef](#)]
25. Chippar, P.; Ju, H. Evaluating cold-start behaviors of end and intermediate cells in a polymer electrolyte fuel cell (PEFC) stack. *Solid State Ionics* **2012**, *225*, 85–91. [[CrossRef](#)]
26. Shaygan, M.; Ehyaei, M.A.; Ahmadi, A.; Assad, M.E.; Silveira, J.L. Energy, exergy, advanced exergy and economic analyses of hybrid polymer electrolyte membrane (PEM) fuel cell and photovoltaic cells to produce hydrogen and electricity. *J. Clean. Prod.* **2019**, *234*, 1082–1093. [[CrossRef](#)]
27. Liu, P.; Xu, S. A Progress Review on Heating Methods and Influence Factors of Cold Start for Automotive PEMFC System. In Proceedings of the SAE 2020 World Congress Experience, WCX 2020, Detroit, MI, USA, 21–23 April 2020; SAE International: Detroit, MI, USA, 2020.
28. Mehta, V.; Cooper, J.S. Review and analysis of PEM fuel cell design and manufacturing. *J. Power Sources* **2003**, *114*, 32–53. [[CrossRef](#)]
29. Cao, Y.; Li, Y.Q.; Zhang, G.; Jermittiparsert, K.; Nasser, M. An efficient terminal voltage control for PEMFC based on an improved version of whale optimization algorithm. *Energy Rep.* **2020**, *6*, 530–542. [[CrossRef](#)]
30. Chikahisa, T. Microscopic Observations of Freezing Phenomena in PEM Fuel Cells at Cold Starts. *Heat Transf. Eng.* **2013**, *34*, 258–265. [[CrossRef](#)]
31. Wang, Y. Analysis of the key parameters in the cold start of polymer electrolyte fuel cells. *J. Electrochem. Soc.* **2007**, *154*, B1041–B1048. [[CrossRef](#)]
32. Henao, N.; Kelouwani, S.; Agbossou, K.; Dube, Y. Proton exchange membrane fuel cells cold startup global strategy for fuel cell plugin hybrid electric vehicle. *J. Power Sources* **2012**, *220*, 31–41. [[CrossRef](#)]
33. Zhou, Y.B.; Luo, Y.Q.; Yu, S.H.; Jiao, K. Modeling of cold start processes and performance optimization for proton exchange membrane fuel cell stacks. *J. Power Sources* **2014**, *247*, 738–748. [[CrossRef](#)]
34. Zhang, G.B.; Wu, J.T.; Wang, Y.; Yin, Y.; Jiao, K. Investigation of current density spatial distribution in PEM fuel cells using a comprehensively validated multi-phase non-isothermal model. *Int. J. Heat Mass Transf.* **2020**, *150*, 119294. [[CrossRef](#)]